

FAST ALTERNATING VOLUME MAXIMIZATION ALGORITHM FOR BLIND SEPARATION OF NON-NEGATIVE SOURCES

Tsung-Han Chan[†], Chang-Jin Song[†], ArulMurugan Ambikapathi[†], Chong-Yung Chi[†], and Wing-Kin Ma^{*}

[†]Inst. Commun. Eng., National Tsing Hua Univ.
Hsinchu, 30013

E-mail: {tsunghan@mx, cychi@ee}.nthu.edu.tw

^{*}Dept. Electronic Eng., Chinese Univ. Hong Kong
Shatin, N.T., Hong Kong

E-mail: wkma@ieee.org

ABSTRACT

We recently reported an iterative non-negative blind source separation (nBSS) method, called convex analysis of mixtures of non-negative sources via alternating volume maximization (CAMNS-AVM) [1], and demonstrated that it provides promising separation performance in image analysis. Nonetheless, the amount of data may be quite large in practical applications, and this may limit the real-time applicability of CAMNS-AVM. In this paper, we propose a fast CAMNS-AVM algorithm involving three complexity reduction methods, specifically problem equivalence, redundant constraints removal, and customized algorithm implementation. The problem equivalence provides sufficiency in solving one linear program (LP) for each partial volume maximization problem, rather than the two LPs required by the original CAMNS-AVM. Then, we remove redundant constraints of each LP involved in CAMNS-AVM by using Quickhull algorithm to enumerate all the extreme points of the constraint-set-constructed convex hull. Finally, we implement a customized primal-dual interior-point method (IPM) for LP. Some Monte Carlo simulation results demonstrate that the fast CAMNS-AVM algorithm is thirty times more computationally efficient than the original CAMNS-AVM algorithm, without any performance loss.

Index Terms— Non-negative blind source separation, Complexity reduction, Alternating volume maximization, Linear programming, Interior-point method

1. INTRODUCTION

Non-negative blind source separation (nBSS) is a signal processing procedure to separate non-negative source signals from the given observations without any prior information about how the non-negative sources are linearly mixed, and it has been applied to a wide range of science and engineering problems, such as biomedical image analysis [2], hyperspectral image analysis [3], and analytical chemistry [4]. The sources of interest in these real-world applications (e.g., tissue responses and mineral distributions) are in general statistically correlated, which makes the application of most non-negative independent component analysis (ICA) methods ineffective [5, 6]. Advances in nBSS without involving any statistical assumptions include non-negative matrix factorization (NMF) [7] and convex analysis of mixtures of non-negative sources (CAMNS) [1, 8], to name a few. NMF may suffer from non-unique decomposition issues [7] and some remedies by considering the sparseness of the sources were

reported in [9]. CAMNS [1, 8] is a convex geometry based framework, where the nBSS problem is formulated as a problem of finding the extreme points of an observation-constructed polyhedral set. Two methods for practically locating the extreme points were reported [1, 8]. One is called CAMNS-LP [8] that uses linear program (LP) and the orthogonal projection to find the extreme points in a systematic manner, while the other called CAMNS via alternating volume maximization (CAMNS-AVM) [1] shows better robustness against model mismatches than CAMNS-LP. However, in practical applications, the size of the data to be processed may be quite large, and thus hinder their real-time applicability.

In this paper, three complexity reduction methods, namely problem equivalence, redundant constraints removal, and customized algorithm implementation, are proposed for improving the speed of CAMNS-AVM algorithm. In the original CAMNS-AVM [1], the volume maximization problem can be handled by alternating optimization, and each associated partial maximization problem requires solving two linear programs (LPs). We first show that the volume maximization problem has an equivalent problem, by virtue of which each partial maximization problem involves solving one LP to obtain the global optimal solution of the original partial maximization problem. Furthermore, because each LP considered may involve lots of redundant linear inequality constraints, the second method is to remove those redundant constraints. We first transform the constraint set into an equivalent convex hull representation, by virtue of which the redundant constraint removal problem is converted into an extreme point enumeration problem. Then, the extreme points can be identified by the well-known Quickhull algorithm [10]. The third method is to implement a customized primal-dual interior-point method (IPM) for solving LPs. Finally, some simulation results demonstrate the computation efficiency of the proposed fast CAMNS-AVM over the original CAMNS-AVM.

Notations: $\mathbf{1}_N$, \mathbf{I}_N , and \mathbf{e}_i represent the $N \times 1$ all-one vector, the $N \times N$ identity matrix, and the unit column vector with the i th entry equal to 1, respectively; “ \succeq ”, “ \circ ”, and “ $\|\cdot\|_2$ ” stand for componentwise inequality, Hadamard product, and Euclidean norm, respectively; \mathbf{x}^{-1} and $[\mathbf{x}]_i$ denote the componentwise inverse of \mathbf{x} and the i th element of \mathbf{x} , respectively; $\text{diag}(\mathbf{x})$ is the diagonal matrix with its diagonal entries being the elements of \mathbf{x} and $\det(\mathbf{X})$ denotes the determinant of the square matrix \mathbf{X} .

2. REVIEW OF CAMNS-AVM ALGORITHM

Consider a scenario that there are M noise-free observations which are linearly mixed from N sources, as given below:

$$\mathbf{x}_i = \sum_{j=1}^N a_{ij} \mathbf{s}_j, \quad i = 1, \dots, M, \quad (1)$$

This work is supported by the National Science Council under Grants NSC 99-2221-E-007-003-MY3, and by a General Research Fund of Hong Kong Research Grant Council (Project No. CUHK415509).

where a_{ij} denotes the unknown mixing coefficient between the i th observation $\mathbf{x}_i = [x_i[1], \dots, x_i[L]]^T$ and the j th source $\mathbf{s}_j = [s_j[1], \dots, s_j[L]]^T$, and $L \gg \max\{M, N\}$ is the data length.

The goal of CAMNS-AVM is to estimate the sources $\mathbf{s}_1, \dots, \mathbf{s}_N$ from the given observations $\mathbf{x}_1, \dots, \mathbf{x}_M$, assuming prior knowledge of N given and under the following assumptions:

- (A1) For all $j = 1, \dots, N$, $\mathbf{s}_j \succeq \mathbf{0}$.
- (A2) For each $i \in \{1, \dots, N\}$, there exists an (unknown) index ℓ_i such that $s_i[\ell_i] > 0$ and $s_j[\ell_i] = 0, \forall j \neq i$.
- (A3) For all $i = 1, \dots, M$, $\sum_{j=1}^N a_{ij} = 1$.
- (A4) $M \geq N$ and $\mathbf{A} \triangleq [a_{ij}]_{M \times N}$ is of full column rank.

Assumption (A1) holds true for image signals. Assumption (A2) is valid for high contrast source images, especially with applications in biomedical image analysis [2]. Assumption (A3) is automatically satisfied in magnetic resonance imaging (MRI) due to the partial volume effect [2]. When violated, (A3) can be enforced through sum-based normalization [8]. Assumption (A4) is a general assumption in nBSS.

Next, we briefly review the CAMNS criterion [1, 8] and the CAMNS-AVM [1].

2.1. CAMNS Criterion

We first construct the polyhedral set \mathcal{S} from the observations as follows:

$$\mathcal{S} = \{ \mathbf{x} \in \mathbb{R}^L \mid \mathbf{x} = \mathbf{C}\boldsymbol{\alpha} + \mathbf{d} \succeq \mathbf{0}, \boldsymbol{\alpha} \in \mathbb{R}^{N-1} \} \quad (2)$$

where \mathbf{C} and \mathbf{d} are given by

$$\mathbf{d} = \frac{1}{M} \sum_{i=1}^M \mathbf{x}_i, \quad \mathbf{C} = [\mathbf{q}_1(\mathbf{U}\mathbf{U}^T), \dots, \mathbf{q}_{N-1}(\mathbf{U}\mathbf{U}^T)] \quad (3)$$

in which $\mathbf{U} = [\mathbf{x}_1 - \mathbf{d}, \dots, \mathbf{x}_M - \mathbf{d}] \in \mathbb{R}^{L \times M}$ and $\mathbf{q}_i(\mathbf{U}\mathbf{U}^T)$ denotes the unit-norm eigenvector associated with the i th principal eigenvalue of $\mathbf{U}\mathbf{U}^T$. Under assumptions (A1)-(A4), it has been shown in [8] that \mathcal{S} is identical to the source convex hull; i.e.,

$$\mathcal{S} = \text{conv}\{\mathbf{s}_1, \dots, \mathbf{s}_N\} \triangleq \left\{ \mathbf{s} = \sum_{i=1}^N \theta_i \mathbf{s}_i \mid \boldsymbol{\theta} \succeq \mathbf{0}, \mathbf{1}_N^T \boldsymbol{\theta} = 1 \right\},$$

where $\boldsymbol{\theta} = [\theta_1, \dots, \theta_N]^T$. A point $\mathbf{x} \in \text{conv}\{\mathbf{s}_1, \dots, \mathbf{s}_N\}$ is called an extreme point of $\text{conv}\{\mathbf{s}_1, \dots, \mathbf{s}_N\}$ if it cannot be a nontrivial convex combination of $\mathbf{s}_1, \dots, \mathbf{s}_N$; i.e.,

$$\mathbf{x} \neq \sum_{i=1}^N \theta_i \mathbf{s}_i \quad (4)$$

for all $\boldsymbol{\theta} \succeq \mathbf{0}$, $\mathbf{1}_N^T \boldsymbol{\theta} = 1$, and $\boldsymbol{\theta} \neq \mathbf{e}_i$ for any i . It has also been shown in [8] that the N extreme points of \mathcal{S} are exactly the true sources $\mathbf{s}_1, \dots, \mathbf{s}_N$. This has led to the following nBSS criterion:

CAMNS criterion [8]: Find all the N extreme points of the polyhedral set \mathcal{S} in (2). Output the obtained extreme points $\{\hat{\mathbf{s}}_1, \dots, \hat{\mathbf{s}}_N\}$ as the estimated sources.

In [8], we have developed CAMNS-LP to enumerate the N extreme points of \mathcal{S} in a systematic manner.

To shed some light into the CAMNS-AVM algorithm [1] which offers better robustness against model mismatch with (A2) than

CAMNS-LP, the pre-image of \mathcal{S} under the affine mapping $\mathbf{x} = \mathbf{C}\boldsymbol{\alpha} + \mathbf{d}$ is considered:

$$\mathcal{F} = \{ \boldsymbol{\alpha} \in \mathbb{R}^{N-1} \mid \mathbf{C}\boldsymbol{\alpha} + \mathbf{d} \succeq \mathbf{0} \} \quad (5a)$$

$$= \{ \boldsymbol{\alpha} \in \mathbb{R}^{N-1} \mid \mathbf{c}_n^T \boldsymbol{\alpha} + d_n \geq 0, n = 1, \dots, L \}, \quad (5b)$$

where \mathbf{c}_n^T is the n th row vector of \mathbf{C} and d_n is the n th element of \mathbf{d} . There exists a one-to-one mapping between extreme points of \mathcal{S} and \mathcal{F} [8], as stated below:

Alternative CAMNS criterion [8]: Find all the N extreme points of the polyhedral set \mathcal{F} given by (5a) and denote the obtained extreme points by $\{\hat{\boldsymbol{\alpha}}_1, \dots, \hat{\boldsymbol{\alpha}}_N\}$. Output

$$\hat{\mathbf{s}}_i = \mathbf{C}\hat{\boldsymbol{\alpha}}_i + \mathbf{d}, \quad i = 1, \dots, N, \quad (6)$$

as the estimated sources.

Figure 1 illustrates the one-to-one affine mapping between the vectors in \mathcal{S} and \mathcal{F} for $N = 3$. The polyhedral sets \mathcal{S} and \mathcal{F} , respectively, contain only N extreme points under assumptions (A1)-(A4). Nevertheless, in practical scenarios where the assumption (A2) is not perfectly satisfied, the number of extreme points in \mathcal{F} could be more than N . A pictorial illustration of such a case is given in Figure 2. One can see that the polyhedral set \mathcal{F} is not a simplex anymore but still exhibits a geometric structure similar to simplex. One would expect that the maximum-volume simplex inside \mathcal{F} could serve as the best approximation to \mathcal{F} [1]. CAMNS-AVM algorithm that finds the N extreme points of the maximum-volume simplex within \mathcal{F} will be briefly reviewed.

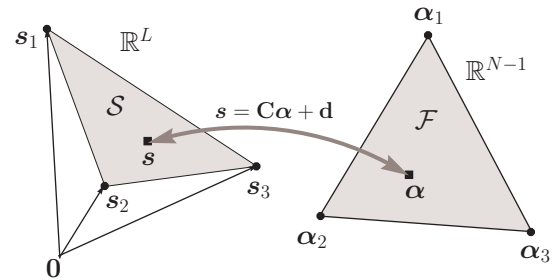


Fig. 1. A geometrical illustration of the one-to-one mapping between \mathcal{S} and \mathcal{F} for $N = 3$ under assumptions (A1)-(A4).

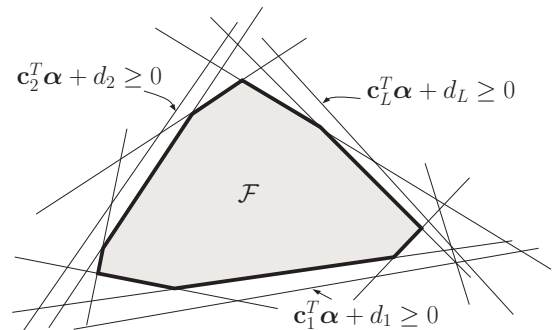


Fig. 2. A geometrical illustration of \mathcal{F} for $N = 3$ and when assumption (A2) is not perfectly satisfied.

2.2. Alternating Volume Maximization for CAMNS

The volume maximization problem is formulated as follows [1]:

$$\begin{aligned} \{\beta_1^*, \dots, \beta_N^*\} &= \arg \max_{\beta_1, \dots, \beta_N \in \mathcal{F}} \text{vol}(\beta_1, \dots, \beta_N) \quad (7) \\ &\equiv \arg \max_{\beta_1, \dots, \beta_N \in \mathcal{F}} |\det(\Delta(\beta_1, \dots, \beta_N))|, \quad (8) \end{aligned}$$

where $\text{vol}(\beta_1, \dots, \beta_N)$ is the volume of $\text{conv}\{\beta_1, \dots, \beta_N\}$ [11],

$$\Delta(\beta_1, \dots, \beta_N) = \begin{bmatrix} \beta_1 & \cdots & \beta_N \\ 1 & \cdots & 1 \end{bmatrix} \in \mathbb{R}^{N \times N}, \quad (9)$$

and $\{\beta_1^*, \dots, \beta_N^*\}$ is the estimate of the set of extreme points $\{\alpha_1, \dots, \alpha_N\}$.

Problem (8) is a difficult, nonconvex problem, but it can be handled by alternating optimization. Consider the cofactor expansion for $\det(\Delta(\beta_1, \dots, \beta_N))$ along the j th column for any $j \in \{1, \dots, N\}$:

$$\det(\Delta(\beta_1, \dots, \beta_N)) = \mathbf{b}_j^T \beta_j + (-1)^{N+j} \det(\mathcal{B}_{Nj}) \quad (10)$$

where $\mathbf{b}_j = [(-1)^{i+j} \det(\mathcal{B}_{ij})]_{i=1}^{N-1}$ and \mathcal{B}_{ij} is the submatrix of $\Delta(\beta_1, \dots, \beta_N)$ with i th row and j th column removed. The partial maximization with respect to β_j with all the other β_i s fixed is expressed as follows:

$$\max_{\beta_j \in \mathcal{F}} |\mathbf{b}_j^T \beta_j + (-1)^{N+j} \det(\mathcal{B}_{Nj})|. \quad (11)$$

Such a partial maximization problem can be globally solved by the following two LPs:

$$p^* = \max_{\beta_j \in \mathcal{F}} \mathbf{b}_j^T \beta_j + (-1)^{N+j} \det(\mathcal{B}_{Nj}), \quad (12a)$$

$$q^* = \min_{\beta_j \in \mathcal{F}} \mathbf{b}_j^T \beta_j + (-1)^{N+j} \det(\mathcal{B}_{Nj}). \quad (12b)$$

The optimal solution of (11) is chosen as the optimal solution of (12a) if $|p^*| > |q^*|$, and is that of (12b) if $|q^*| > |p^*|$. Problem (12) can be implemented by available LP solvers, such as SeDuMi [12] and CVX [13]. The partial maximization problem (12) is solved cyclically (i.e., $j := (j \text{ modulo } N) + 1$) until some predefined stopping rule is satisfied. Here, each cycle corresponds to an update of $\{\beta_1, \dots, \beta_N\}$. Denoting the outcome of the above described alternating volume maximization process by $\{\hat{\beta}_1, \dots, \hat{\beta}_N\}$, the sources can be estimated by

$$\hat{\mathbf{s}}_j = \mathbf{C} \hat{\beta}_j + \mathbf{d}. \quad (13)$$

The CAMNS-AVM algorithm is summarized in Table 1.

3. FAST CAMNS-AVM ALGORITHM

In this section, we propose three complexity reduction methods for CAMNS-AVM (respectively in each subsection) so that its computational efficiency can be significantly improved.

3.1. Volume maximization problem equivalence

We first show the Problem (8) can be simplified. By basic matrix analysis, $\det(\mathbf{G}) = -\det(\mathbf{H})$ if \mathbf{H} results from \mathbf{G} by interchanging any two column or row vectors. Then, an optimal solution of (8) such that $\det(\Delta(\beta_1^*, \dots, \beta_N^*)) \geq 0$ always exists. Problem (8) therefore can be simplified to

$$\max_{\beta_1, \dots, \beta_N \in \mathcal{F}} \det(\Delta(\beta_1, \dots, \beta_N)). \quad (14)$$

Table 1. CAMNS-AVM algorithm.

Given a convergence tolerance $\varepsilon > 0$, \mathbf{C} and \mathbf{d} obtained by (3), and the set of dimension-reduced observations $\mathcal{X} = \{\mathbf{C}^T(\mathbf{x}_i - \mathbf{d}), i = 1, \dots, M\}$.

Step 1. initialize β_1, \dots, β_N by randomly choosing N vectors from \mathcal{X} , compute $\varrho := |\det(\Delta(\beta_1, \dots, \beta_N))|$, and set $j := 1$.

Step 2. update $\mathbf{b}_j := [(-1)^{i+j} \det(\mathcal{B}_{ij})]_{i=1}^{N-1}$ where \mathcal{B}_{ij} is a submatrix of $\Delta(\beta_1, \dots, \beta_N)$ with the i th row and j th column removed.

Step 3. solve the LPs (12a) and (12b) by SeDuMi [12] or CVX [13] and obtain their optimal solutions, denoted by $\bar{\beta}_j$ and $\underline{\beta}_j$, respectively.

Step 4. if $|p^*| > |q^*|$, then update $\beta_j := \bar{\beta}_j$; otherwise, update $\beta_j := \underline{\beta}_j$.

Step 5. if $(j \text{ modulo } N) \neq 0$, then $j := j + 1$, and go to **Step 2**, else compute $\varrho' := |\det(\Delta(\beta_1, \dots, \beta_N))|$,
if $|\varrho' - \varrho|/\varrho < \varepsilon$, then $\hat{\beta}_i = \beta_i$ for $i = 1, \dots, N$,
otherwise, set $\varrho' := \varrho, j := 1$, and go to **Step 2**.

Step 6. output the source estimates $\hat{\mathbf{s}}_j = \mathbf{C} \hat{\beta}_j + \mathbf{d}, j = 1, \dots, N$.

By the cofactor expansion for $\det(\Delta(\beta_1, \dots, \beta_N))$ in (10), the partial maximization problem associated with (14) can be solved by considering only (12a) rather than by the two LPs (12a) and (12b) in the original CAMNS-AVM. In the next two subsections, we will present how the computational complexity in solving the LP in (12a) can be further reduced.

3.2. Removal of Redundant Constraints

As observed in Figure 2, the polyhedral set \mathcal{F} is the set of intersection of L halfspaces, in which there may exist many redundant constraints. We derive an equivalent representation of \mathcal{F} that involves a much less amount of inequality constraints, as described in the following proposition:

Proposition 1. The polyhedral set \mathcal{F} given by (5a) is identical to

$$\mathcal{F} = \{\alpha \in \mathbb{R}^{N-1} \mid \bar{\mathbf{C}}\alpha + \bar{\mathbf{d}} \succeq \mathbf{0}\}, \quad (15)$$

where $\bar{\mathbf{C}} = [\mathbf{c}_{i_1}, \dots, \mathbf{c}_{i_r}]^T$ and $\bar{\mathbf{d}} = [d_{i_1}, \dots, d_{i_r}]^T$. Here, $\{\mathbf{c}_{i_1}/d_{i_1}, \dots, \mathbf{c}_{i_r}/d_{i_r}\}$ is the set of the extreme points of $\text{conv}\{\mathbf{c}_1/d_1, \dots, \mathbf{c}_L/d_L\}$ and r is the number of its extreme points.

The proof of Proposition 1 is given in Appendix. Proposition 1 transforms the problem of redundant constraints removal for \mathcal{F} to the problem of finding extreme points of $\text{conv}\{\mathbf{c}_1/d_1, \dots, \mathbf{c}_L/d_L\}$, or known as the extreme point enumeration problem in the optimization literature.

Extreme point enumeration has been widely investigated in the past three decades [14]. The complexity of the existing extreme point enumeration algorithms would increase exponentially with the number of data points. Nevertheless, Quickhull, a well-known point enumeration algorithm [10], has been found to be computationally efficient in many practical applications [15]. In our simulations to be presented in Section 4, we use Quickhull algorithm to find the extreme points of $\text{conv}\{\mathbf{c}_1/d_1, \dots, \mathbf{c}_L/d_L\}$, and the extra computation time overhead of Quickhull is also taken into account while calculating the total time consumption of the proposed fast CAMNS-AVM algorithm.

3.3. Customized Primal-dual Interior-Point Method for LP

Our aim herein is to develop a customized LP solver for Problem (12a) that enables self-defined initialization, which is not an available option for general-purpose solvers such as SeDuMi and CVX [12, 13]. The development is based on the primal-dual IPM by S. Boyd *et al.* [16, Chapter 11.7]. By Proposition 1, the LP in (12a) is equivalent to

$$\begin{aligned} \min_{\beta_j} \quad & -\mathbf{b}_j^T \beta_j \\ \text{s.t.} \quad & -\bar{\mathbf{C}}\beta_j - \bar{\mathbf{d}} \preceq \mathbf{0}, \end{aligned} \quad (16)$$

where $(-1)^{N+j} \det(\mathbf{B}_{Nj})$ is ignored since \mathbf{B}_{Nj} does not depend on β_j . The IPM iteratively updates the primal-dual variable (β_j, λ) by $(\beta_j + \gamma\Delta\beta_j, \lambda + \gamma\Delta\lambda)$ where $(\Delta\beta_j, \Delta\lambda)$ and γ denote the search direction and the step size, respectively. By solving the modified Karush-Kuhn-Tucker (KKT) conditions with the first-order approximation, $(\Delta\beta_j, \Delta\lambda)$ can be obtained as follows:

$$\Delta\beta_j = (\bar{\mathbf{C}}^T \mathbf{D} \bar{\mathbf{C}})^{-1} (\bar{\mathbf{C}}^T \mathbf{D} \mathbf{r}_2 - \mathbf{r}_1), \quad (17a)$$

$$\Delta\lambda = \mathbf{D}(\mathbf{r}_2 - \bar{\mathbf{C}}\Delta\beta_j), \quad (17b)$$

where

$$\mathbf{D} = \text{diag}(\lambda \circ (\bar{\mathbf{C}}\beta_j + \bar{\mathbf{d}})^{-1}), \quad (18)$$

$$\mathbf{r}_1 = -\mathbf{b}_j - \bar{\mathbf{C}}^T \lambda, \quad (19)$$

$$\mathbf{r}_2 = -(\bar{\mathbf{C}}\beta_j + \bar{\mathbf{d}}) + (1/t)\lambda^{-1}, \quad t > 0. \quad (20)$$

The step size $\gamma \in (0, 1]$ can be chosen as any value such that $\lambda + \gamma\Delta\lambda \succ \mathbf{0}$ and $\bar{\mathbf{C}}(\beta_j + \gamma\Delta\beta_j) + \bar{\mathbf{d}} \succ \mathbf{0}$. We first compute the corresponding largest step size γ as follows

$$\begin{aligned} \hat{\gamma} &= \sup\{\gamma \in (0, 1] \mid \lambda + \gamma\Delta\lambda \succ \mathbf{0}, \bar{\mathbf{C}}(\beta_j + \gamma\Delta\beta_j) + \bar{\mathbf{d}} \succ \mathbf{0}\} \\ &= \min \left\{ 1, \min \left\{ -\frac{[\lambda]_i}{[\Delta\lambda]_i} \mid [\Delta\lambda]_i < 0 \right\}, \right. \\ &\quad \left. \min \left\{ -\frac{[\bar{\mathbf{C}}\beta_j + \bar{\mathbf{d}}]_i}{[\bar{\mathbf{C}}\Delta\beta_j]_i} \mid [\bar{\mathbf{C}}\Delta\beta_j]_i < 0 \right\} \right\}. \end{aligned} \quad (21)$$

Then, a step size can be determined as $\gamma = 0.99\hat{\gamma}$ to ensure $\lambda + \gamma\Delta\lambda \succ \mathbf{0}$ and $\bar{\mathbf{C}}(\beta_j + \gamma\Delta\beta_j) + \bar{\mathbf{d}} \succ \mathbf{0}$. With the duality gap setting as given in [16], the customized IPM for (16) is described in Table 2.

Table 2. Customized primal-dual IPM for (16).

Given	a primal-dual strictly feasible initial point (β_j, λ) , $\mu = 10$, and a solution accuracy $\epsilon > 0$.
Step 1.	calculate the surrogate duality gap $\hat{\eta}(\beta_j, \lambda) = (\bar{\mathbf{C}}\beta_j + \bar{\mathbf{d}})^T \lambda$ and determine $t := \mu r / \hat{\eta}(\beta_j, \lambda)$.
Step 2.	compute $(\Delta\beta_j, \Delta\lambda)$ given by (17).
Step 3.	compute $\hat{\gamma}$ by (21) and the step size $\gamma = 0.99\hat{\gamma}$.
Step 4.	update $\beta_j := \beta_j + \gamma\Delta\beta_j$ and $\lambda := \lambda + \gamma\Delta\lambda$.
Step 5.	go to Step 1 until $\hat{\eta}(\beta_j, \lambda) \leq \epsilon$.

With all the above complexity reduction methods applied to CAMNS-AVM, we come up with the fast CAMNS-AVM algorithm given in Table 3. The key differences between the original CAMNS-AVM and the fast CAMNS-AVM lie in Step 1 and Step 4 (in Table 3), which are elaborated in the following remarks:

- (R1) Step 1 is to remove the redundant constraints in \mathcal{F} . Since \mathcal{F} , represented by $(\bar{\mathbf{C}}, \bar{\mathbf{d}})$ (by Proposition 1), is uniquely determined by only $r \ll L$ linear inequalities, the complexity of each partial maximization problem (12a) can be significantly reduced.
- (R2) Step 4 involves two computational efficiency improvements. One is that we only need to solve one LP (16) rather than two LPs (12) required in the original CAMNS-AVM (see Step 3 in Table 1). This implies that the complexity of CAMNS-AVM can be reduced by one half. Moreover, the optimal β_j obtained by the customized LP at the current cycle can be used to initialize the LP at the next cycle. This mechanism is called the warm start which further accelerates CAMNS-AVM.

Table 3. Fast CAMNS-AVM algorithm.

Given	a convergence tolerance $\epsilon > 0$, \mathbf{C} and \mathbf{d} obtained by (3), and the set $\mathcal{X} = \{ \mathbf{C}^T(\mathbf{x}_i - \mathbf{d}), i = 1, \dots, M \}$.
Step 1.	obtain $(\bar{\mathbf{C}}, \bar{\mathbf{d}})$ by Quickhull [10] as presented in Section 3.2.
Step 2.	initialize β_1, \dots, β_N by randomly choosing N vectors from \mathcal{X} , compute $\varrho := \det(\Delta(\beta_1, \dots, \beta_N))$, and set $j := 1$.
Step 3.	update $\mathbf{b}_j := [(-1)^{i+j} \det(\mathbf{B}_{ij})]_{i=1}^{N-1}$ where \mathbf{B}_{ij} is a submatrix of $\Delta(\beta_1, \dots, \beta_N)$ with the i th row and j th column removed.
Step 4.	solve the LP (16) by the customized primal-dual IPM (Table 2) with the iterate β_j at the previous cycle and $\lambda = (\bar{\mathbf{C}}\beta_j + \bar{\mathbf{d}})^{-1}$ as the initial points to obtain an optimal solution β_j .
Step 5.	if $(j \bmod N) \neq 0$, then $j := j + 1$, and go to Step 3 , else compute $\varrho' := \det(\Delta(\beta_1, \dots, \beta_N))$, if $ \varrho' - \varrho /\varrho < \epsilon$, then $\hat{\beta}_i = \beta_i$ for $i = 1, \dots, N$, otherwise, set $\varrho' := \varrho, j := 1$, and go to Step 3 .
Step 6.	output the source estimates $\hat{\mathbf{s}}_j = \mathbf{C}\hat{\beta}_j + \mathbf{d}, j = 1, \dots, N$.

4. SIMULATIONS

A Monte Carlo simulation with 100 independent runs is presented to demonstrate the proposed fast CAMNS-AVM. In each run, we synthetically generated 7 mixtures from 7 human face images ($M = N = 7$ and $L = 76800$), taken from [1]. A sum square error (SSE) between $\hat{\mathbf{s}}_i$ and \mathbf{s}_i is used as the performance measure [1]:

$$\text{SSE} = \min_{\pi \in \Pi_N} \sum_{i=1}^N \left\| \mathbf{s}_i - \frac{\|\mathbf{s}_i\|_2}{\|\hat{\mathbf{s}}_{\pi_i}\|_2} \hat{\mathbf{s}}_{\pi_i} \right\|_2^2 \quad (22)$$

where $\pi = (\pi_1, \dots, \pi_N)$, and $\Pi_N = \{\pi \in \mathbb{R}^N \mid \pi_i \in \{1, 2, \dots, N\}, \pi_i \neq \pi_j \text{ for } i \neq j\}$ is the set of all the permutations of $\{1, 2, \dots, N\}$. In addition, the computation time T (in secs) of the method (implemented in Mathworks Matlab R2008a) running on a desktop computer equipped with Core 2 Duo CPU 2.33GHz, 4GB memory is used as our computational complexity measure.

The average SSE and computation time T per realization are shown in Table 4. In Case A, the original CAMNS-AVM (in Table 1) is used. In Case B, we consider the CAMNS-AVM with Steps 3 and 4 (in Table 1) replaced by solving (12a) only. Case C is similar to Case B except that in Case C(i), (12a) is solved by the customized IPM and in Case C(ii), \mathcal{F} given by (12a) is further replaced by (15), found by Quickhull [10]. Finally, Case D is for the fast CAMNS-AVM (given in Table 3). One can see that the average SSEs are the same for all the cases, and the computational efficiency literally improves from Case A to Case D. In particular, the computation time

Table 4. The average SSE and the computation time T per realization for performance and complexity comparison of the original CAMNS-AVM (Case A) with different complexity reduction methods used (Cases B, C, and D), where Case D is the proposed fast CAMNS-AVM algorithm.

Methods		number of constraints	SSE (dB)	T (secs)
Case A:	Original CAMNS-AVM -using SeDuMi to solve 2 LPs in (12)	$L = 76800$	17.46	103.22
Case B:	CAMNS-AVM -using SeDuMi to solve 1 LP in (12a)	$L = 76800$	17.46	59.33
Case C:	(i) CAMNS-AVM -using customized IPM to solve (12a)	$L = 76800$	17.46	22.82
	(ii) CAMNS-AVM -using Quickhull to find (15) and SeDuMi to solve (12a)	$r = 976$	17.46	4.39
Case D:	Fast CAMNS-AVM -using Quickhull to find (15) and customized IPM to solve (12a)	$r = 976$	17.46	3.27

T in Case B is almost twice less than that in Case A. By using the customized IPM and the warm start mechanism, the computation time T in Case C(i) is more than twice less than that in Case B, while the computation time T in Case C(ii) is significantly smaller than that in Case B, because all the redundant inequality constraints $((L - r)/L \approx 98.73\%)$ in \mathcal{F} have been removed. The computation time T in Case D is less than that in Case C(i) and Case C(ii) by around 19 and 1 seconds, respectively. As a result, the total computation time of the proposed fast CAMNS-AVM (Case D) is more than thirty times less than that of the original CAMNS-AVM (Case A). Let us emphasize again that the computation time overhead required by Quickhull algorithm has been incorporated in whole computation time calculation for Case C and Case D.

One typical realization among the 100 independent runs is shown in Figure 3, where all of the separated images have been properly ordered for ease of visual comparison. One can see that the images extracted by the original CAMNS-AVM and the proposed fast CAMNS-AVM are exactly the same, which again validates that the fast CAMNS-AVM algorithm achieves the same performance with much less computation time.

5. CONCLUSION

We have proposed a fast CAMNS-AVM algorithm given in Table 3 which employs the three computational complexity reduction methods, namely problem equivalence, redundant constraints removal, and customized IPM implementation, to reduce the computational complexity of the original CAMNS-AVM without any performance loss. The presented simulation results have shown that any combinations of the three proposed complexity reduction methods can improve the computational efficiency of the original CAMNS-AVM, and the proposed fast CAMNS-AVM algorithm (with all the three proposed methods applied) is much faster (thirty times) than the original CAMNS-AVM. From the algorithm implementation point of view, the former is therefore much more suitable for practical applications than the latter in spite of the same performance.

6. APPENDIX

Since $\mathbf{x}_i \succeq \mathbf{0}$, $\forall i$ in image applications and the data where $x_i[r_i] = 0$, $\forall i$ can be removed without loss of practicality, we have $\mathbf{d} \succ \mathbf{0}$ by (3). Then, an equivalent form of (5b) can be written as

$$\mathcal{F} = \{\boldsymbol{\alpha} \in \mathbb{R}^{N-1} \mid \mathbf{v}^T \boldsymbol{\alpha} \leq 1, \mathbf{v} \in \mathcal{V}\}, \quad (23)$$

where $\mathbf{v}_n = -\mathbf{c}_n/d_n$ and $\mathcal{V} = \{\mathbf{v}_1, \dots, \mathbf{v}_L\}$. It has been pointed out in [17] that \mathcal{F} is known as the polar dual of \mathcal{V} . Hence, we have

the following property

Property 1. ([17]) *A vector $\mathbf{v}_n \in \mathcal{V}$ is (not) an extreme point of $\text{conv}\{\mathcal{V}\}$ if and only if $\mathbf{v}_n^T \boldsymbol{\alpha} \leq 1$ is active (redundant) in \mathcal{F} . Suppose that $\mathbf{v}_{l_1}, \dots, \mathbf{v}_{l_r}$ are the extreme points of $\text{conv}\{\mathcal{V}\}$. By (23) and Property 1, \mathcal{F} can be fully represented by the active constraints; i.e.,*

$$\mathcal{F} = \{\boldsymbol{\alpha} \in \mathbb{R}^{N-1} \mid \mathbf{v}^T \boldsymbol{\alpha} \leq 1, \mathbf{v} \in \{\mathbf{v}_{l_1}, \dots, \mathbf{v}_{l_r}\}\}. \quad (24)$$

Hence, (15) directly follows from (24). \blacksquare

7. REFERENCES

- [1] W.-K. Ma, T.-H. Chan, C.-Y. Chi, and Y. Wang, "Convex analysis for non-negative blind source separation with application in imaging," in Chapter 7, *Convex Optimization in Signal Processing and Communications*, Editors: D. P. Palomar and Y. C. Eldar, UK: Cambridge University Press, 2010.
- [2] Y. Wang, J. Xuan, R. Srikanthana, and P. L. Choyke, "Modeling and reconstruction of mixed functional and molecular patterns," *Intl. J. of Biomed. Imag.*, vol. 2006, pp. 1–9, 2006.
- [3] N. Keshava and J. Mustard, "Spectral unmixing," *IEEE Signal Process. Mag.*, vol. 19, no. 1, pp. 44–57, Jan. 2002.
- [4] E. R. Malinowski, *Factor Analysis in Chemistry*, John Wiley, New York, 2002.
- [5] M. D. Plumbley, "Algorithms for non-negative independent component analysis," *IEEE Trans. Neural Netw.*, vol. 14, no. 3, pp. 534–543, 2003.
- [6] S. Moussaoui, D. Brie, A. Mohammad-Djafari, and C. Carteret, "Separation of non-negative mixture of non-negative sources using a Bayesian approach and MCMC sampling," *IEEE Trans. Signal Process.*, vol. 54, no. 11, pp. 4133–4145, Nov. 2006.
- [7] D. Lee and H. S. Seung, "Learning the parts of objects by non-negative matrix factorization," *Nature*, vol. 401, pp. 788–791, Oct. 1999.
- [8] T.-H. Chan, W.-K. Ma, C.-Y. Chi, and Y. Wang, "A convex analysis framework for blind separation of non-negative sources," *IEEE Trans. Signal Process.*, vol. 56, no. 10, pp. 5120–5134, Oct. 2008.
- [9] P. O. Hoyer, "Non-negative matrix factorization with sparseness constraints," *J. of Mach. Learn. Research*, vol. 5, pp. 1457–1469, 2004.
- [10] C. B. Barber, D. P. Dobkin and H. Huhdanpaa, "The quickhull algorithm for convex hulls," *ACM Trans. Math. Software*, vol. 22, pp. 469–483, 1996.

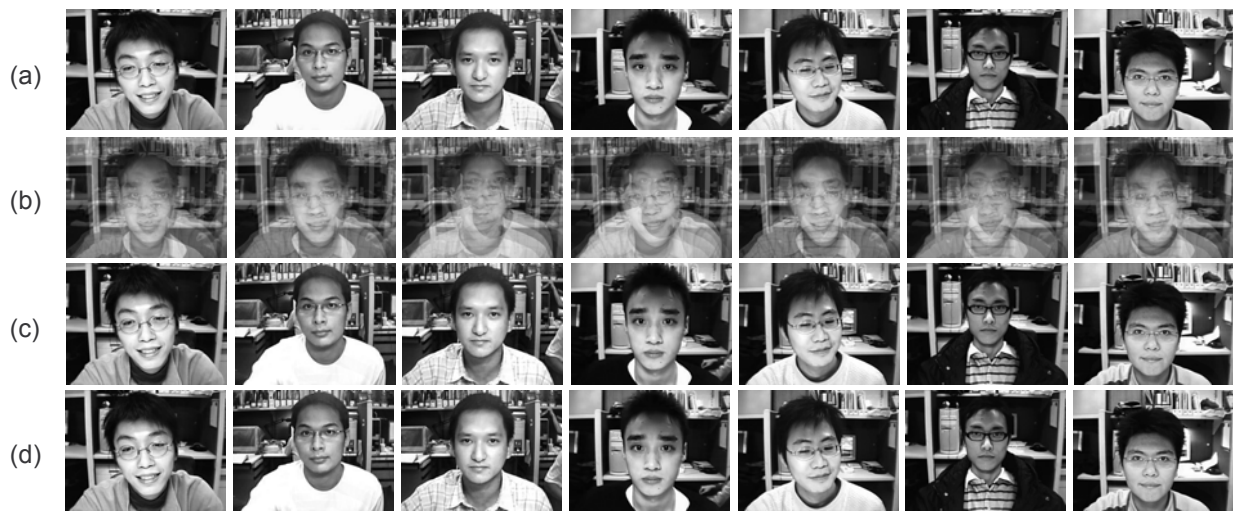


Fig. 3. Human face images: (a) the sources, (b) the observations (mixtures of the sources), and the extracted sources obtained by (c) CAMNS-AVM and (d) fast CAMNS-AVM.

- [11] G. Strang, *Linear Algebra and Its Application*, CA: Thomson, 4th edition, 2006.
- [12] J. F. Sturm, "Using SeDuMi 1.02, a MATLAB toolbox for optimization over symmetric cones," *Optimization Methods and Software*, vol. 11-12, pp. 625–653, 1999.
- [13] M. Grant and S. Boyd, "CVX: Matlab software for disciplined convex programming, version 1.21," <http://cvxr.com/cvx>, Sept. 2010.
- [14] K. G. Murty, "A problem in enumerating extreme points, and an efficient algorithm for one class of polytopes," *Optimization Letters*, vol. 3, no. 2, pp. 211–237, 2009.
- [15] F.-Y. Wang, C.-Y. Chi, T.-H. Chan, and Y. Wang, "Nonnegative least correlated component analysis for separation of dependent sources by volume maximization," *IEEE Trans. Pattern Analysis and Machine Intelligence*, vol. 32, no. 5, pp. 875-888, May 2010.
- [16] S. Boyd and L. Vandenberghe, *Convex Optimization*, Cambridge Univ. Press, 2004.
- [17] S. Jibrin, A. Boneh, and R. J. Caron, "Probabilistic algorithms for extreme point identification," *Journal of Interdisciplinary Mathematics*, vol. 10, pp. 131–142, 2007.